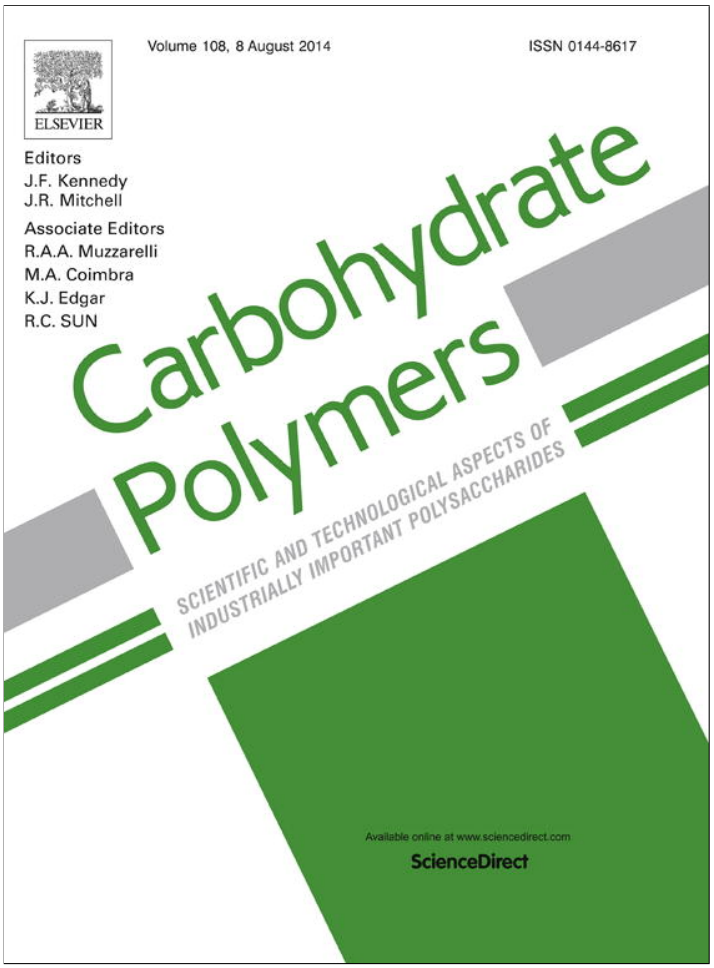

Carbohydrate Polymers 108 (2014) 232–238

Contents lists available at ScienceDirect

Carbohydrate Polymers

journal homepage: www.elsevier.com/locate/carbpol

Porous starch/cellulose nanofibers composite prepared by salt leaching technique for tissue engineering

Bijan Nasri-Nasrabadi[a], Mohammad Mehrasa[b,*], Mohammad Rafienia[c,*], Shahin Bonakdar[d], Tayebeh Behzad[a], Shahin Gavanji[e]

[a] Department of Chemical Engineering, Isfahan University of Technology, Isfahan 8415681167, Iran
[b] Department of Biotechnology, Faculty of Advanced Sciences and Technologies, University of Isfahan, Isfahan 81746-73441, Iran
[c] Biosensor Research Center, Isfahan University of Medical Sciences, 81744-176 Isfahan, Iran
[d] National Cell Bank of Iran, Pasteur Institute of Iran, 1316943551 Tehran, Iran
[e] Young Researchers Club, Khorasgan Branch, Islamic Azad University, Khorasgan, Isfahan, Iran

ARTICLE INFO

Article history:
Received 29 October 2013
Received in revised form 22 February 2014
Accepted 22 February 2014
Available online 12 March 2014

Keywords:
Starch
Salt leaching
Cellulose
Nanofibers
Tissue engineering

ABSTRACT

Starch/cellulose nanofibers composites with proper porosity pore size, mechanical strength, and biodegradability for cartilage tissue engineering have been reported in this study. The porous thermoplastic starch-based composites were prepared by combining film casting, salt leaching, and freeze drying methods. The diameter of 70% nanofibers was in the range of 40–90 nm. All samples had interconnected porous morphology; however an increase in pore interconnectivity was observed when the sodium chloride ratio was increased in the salt leaching. Scaffolds with the total porogen content of 70 wt% exhibited adequate mechanical properties for cartilage tissue engineering applications. The water uptake ratio of nanocomposites was remarkably enhanced by adding 10% cellulose nanofibers. The scaffolds were partially destroyed due to low in vitro degradation rate after more than 20 weeks. Cultivation of isolated rabbit chondrocytes on the fabricated scaffold proved that the incorporation of nanofibers in starch structure improves cell attachment and proliferation.

1. Introduction

Tissue engineering is an effective and confident method to repair or reestablish injured or destroyed organs. In this approach, scaffold is fabricated in a three-dimensional medium suitable to seed and develop cells (Elisseeff, Puleo, Yang, & Sharma, 2005). Normally, cells are developed on a biodegradable porous scaffold in which the tissue is forming and growing, the scaffold gradually degrades (Khademhosseini & Langer, 2007). In tissue engineering, hydrogels, an important type of biomaterials, consist of a water swollen crosslinked network and high entangled chains which cause low rate of polymer dissolution in water. Due to high oxygen permeability, ease of preparation and suitable viscoelasticity, hydrogels are widely used as a 3D scaffold. Besides, PLA and PVA (synthetic biopolymers), collagen and alginate, the most popular natural polymers, have been used as hydrogels in tissue engineering (Ahearne, Yang, & Liu, 2008; Nguyen & Jennifer, 2002). Starch is a hydrophilic polymer and unique in the case of properties. In addition to porosity controlled by freeze drying and salt leaching, biocompatibility, biodegradability, and acceptable mechanical properties of starch films can create a hydrophilic and porous film classified as a hydrogel in tissue engineering. Starch-based films have a great potential for scaffolds, however, to improve the mechanical properties and regulate the porosity, hydrophilicity, and degradation rate (Hrabalova, 2011; Tiexeira et al., 2010; Wool & Sun, 2005), cellulose nanofibers were added.

In this study, microfibrillated cellulose was individualized from rice straw. Then, starch-cellulose nanofibers composites, in a variety of nanofibers content, were manufactured by film casting. Mechanical properties, water absorption behavior, morphology, and in vitro degradation of samples were investigated.

2. Materials and methods

2.1. Materials

Rice straw was obtained from a local source, (Isfahan, Iran). Modified starch, glycerol, and other chemicals used for chemical

* Corresponding author. Tel.: +98 3117922458.
E-mail addresses: mehrasa.mohammad@yahoo.com (M. Mehrasa), m_rafienia@med.mui.ac.ir, rafie_med@yahoo.com (M. Rafienia).

http://dx.doi.org/10.1016/j.carbpol.2014.02.075
0144-8617/

Table 1
Different formulations of starch based scaffolds.

Scaffold samples	Cellulose nanofibers content (%)	Utilized salt (%)
S/70	0	70
SC5/70	5	70
SC10/70	10	70
SC15/70	15	70
S/90	0	90
SC5/90	5	90
SC10/90	10	90
SC15/90	15	90

purification of fibers were purchased from Merck Company, Germany.

2.2. Preparation of cellulose nanofibers (CNF)

The chemo-mechanical method was applied to extract nanofibers from the rice straw. Dried rice straws, with 4–5 cm length, were soaked in 17.5 wt% NaOH solution for 2 h, and then the fibers were washed with distilled water to naturalize the pH. In order to remove the hemicelluloses, pectin, and semi-crystalline regions, the fibers were hydrolyzed with 2 M HCl solution at 80 ± 5 °C for 2 h and washed with distilled water for several times. The acid hydrolyzed pulp was treated with 2 wt% NaOH solution at 80 ± 5 °C for 2 h to remove the remained hemicelluloses and soluble lignin. The alkali treated fibers were washed repeatedly. The stock was bleached by 20 wt% $NaClO_2$ solution at 50 °C for 1 h to remove the insoluble lignin (Bhatnagar & Sain, 2004). The process of extracting nanofibers was performed by applying a mechanical treatment on the bleached fibers. For this purpose, a dilute suspension (0.05 wt%) of fibers was placed in an ultrasonic generator (at 400 W and 20–25 kHz for 30 min). The ultrasonic treatment was carried out in an ice bath to control the temperature (Chen, Yu, et al., 2011).

2.3. Preparation of starch/cellulose nanofibers composite

The porous starch-based composites, as scaffolds, were prepared by a combination of film casting, salt leaching, and freeze drying methods. The solution containing 90 wt% deionized water, 7 wt% starch and cellulose nanofibers, and 3 wt% glycerol was stirred by a mechanical homogenizer, and heated at 100 °C for 30 min to gelatinize starch (Lu, Weng, & Cao, 2005). The ratios of starch to cellulose nanofibers were selected to be 100/0, 95/5, 90/10, and 85/15. Then, the gelatinized solution was cast into petri dishes on whose surface microparticles of salt (70% and 90% of starch weigh) had been poured. After casting, the salt microparticles were poured on the surface of cast solution as well. The mold was degassed under vacuum at 70 °C. Subsequently, the cast film was dried for 2 days at 40 °C and 50% relative humidity. The final, thickness of starch-based nanocomposites was about 0.3 mm. The prepared film was immersed in deionized water for 3–4 days to leach away the salt and form the porous starch scaffolds. The salt leached samples were placed in a humid chamber (50% relative humidity) for 2 days (Plikk, Malberg, & Albertsson, 2009). In this step, freeze drying (Alpha 1–2 LD model, Christ Co., Germany) was carried out at −80 °C for 2 days under high vacuum. Then, the dried scaffolds were immersed in ethanol (70%, v/v) for 12 h to be sterilized. Before cell culture, the scaffolds were washed several times with phosphate buffer solution (PBS) to remove the residual alcohols (Zhang et al., 2010). Different compositions of starch-based scaffolds are presented in Table 1.

2.4. Morphology

The morphology and dimension of the rice straw and the chemical treated or bleached fibers were characterized by a scanning electron microscopy (SEM) instrument (ZEISS 1450EP, Germany). Dimension of extracted nanofibers after ultrasonication were examined by field emission scanning electron microscopy (FE-SEM) (HITACHI-S4160) and transmission electron microscopy (TEM) (Zeiss model EM 10C, Germany). In order to characterize composites, the specimens were cryo-crushed in liquid nitrogen, and then the morphology of broken surface of scaffolds was studied using SEM.

Porosity percent of scaffolds were obtained from an ethanol displacement method. To this purpose, samples were cut at approximate dimension of 10 × 30 mm and vacuum dried till their weight became kept constant. Samples were then immersed in alcohol to determined scaffolds wet weight (g). The porosity was expressed as follow:

$$\text{Porosity}\% = \frac{V_s - (W_s/\rho)}{V_s} \times 100 \quad (1)$$

where V_s is the total volume of scaffold (cm^3), W_s is the scaffold dry weight, and ρ is the density of dried scaffold (g/cm^3). The measurements were carried out for 5 repetitions to give an average value of the data.

2.5. Chemical analysis

α-Cellulose, hemicelluloses, and lignin contents of untreated and alkali treated fibers were investigated using NREL/TP-510-4268 (NREL, 2008). Also, an improved method was applied to study the effect of chemical purification on silica content of rice straw (Elliott & Snyder, 1991).

2.6. Mechanical analysis

Tensile properties of starch-based scaffolds were evaluated according to ASTM D-638 (TYPV). The measurements were performed at 25 °C and 43% relative humidity using Zwick Universal Testing Machine-1446-60 with a load cell of 10 kN and crashed speed of 5 mm/min. Also, the compressive modulus and strength of samples were measured by MTS instruments (5500 R, US) with a 200 N load cell. The specimens were cut on disk-shape and tests were conducted with a cross-head speed of 0.5 mm/min. For each specimen, five replicates were carried out and the average value was reported.

2.7. Water uptake test

The water uptake measurements were performed following a simple method. The specimens of samples were cut at dimension of 30 × 10 mm, and then soaked in distilled water. The remaining water on the film surfaces was wiped, and the weight of films was measured after 1, 2, 4, 8, 12, and 24 h. The percentage of water absorption was calculated from Eq. (2):

$$\text{Water Absorption}\% = \frac{W_t - W_0}{W_0} \times 100 \quad (2)$$

where W_t and W_0 are the weights at time t and initial weight, respectively (Huang, Ren, Chen, Ren, & Zhou, 2008).

2.8. In vitro degradation

In vitro degradation of the samples was studied in PBS under pH 7.4 and 37 °C. Film specimens (10 mm × 10 mm) were incubated in test tubes containing 15 ml PBS. The tubes were stored

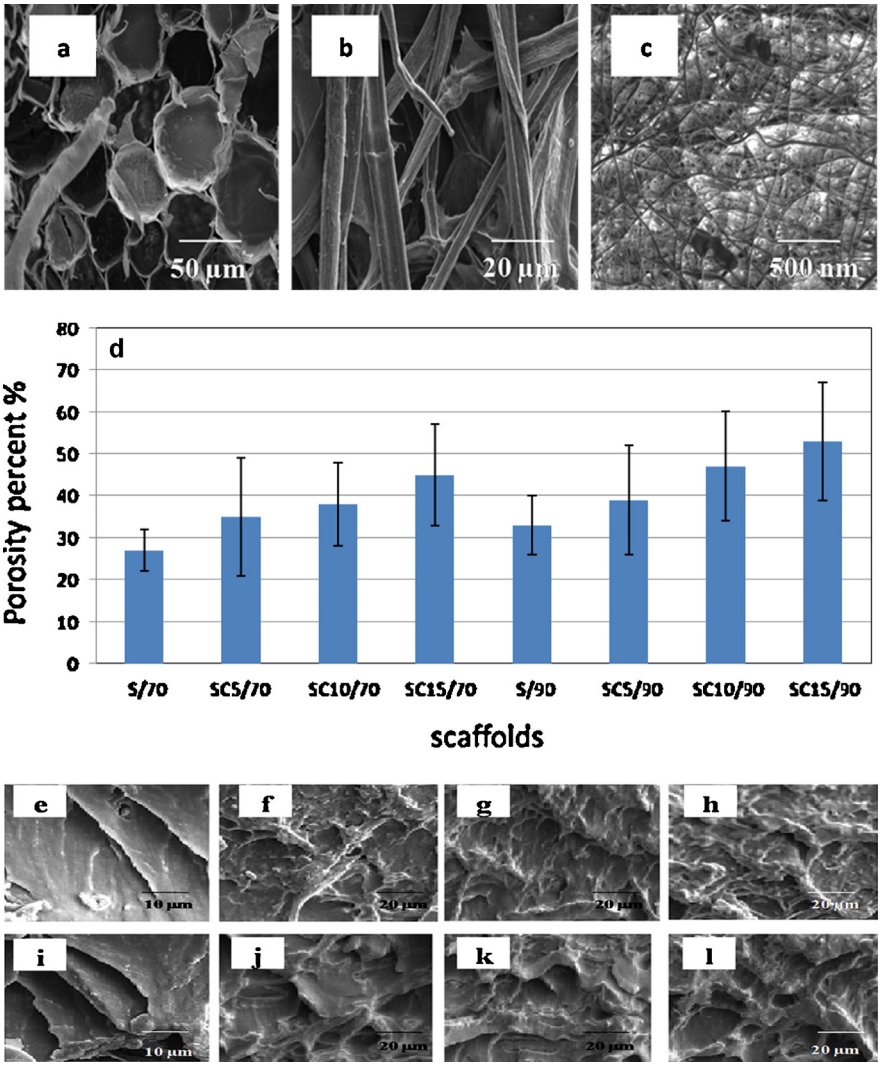

Fig. 1. SEM images of fibers (a) before (cross section), (b) after chemical purification, (c) FE-SEM. (d) The porosity of starch based scaffolds at various salt and nanofibers content. Cross section SEM micrographs of the scaffolds: (e) S/70, (f) SC5/70, (g) SC10/70, (h) SC15/70, (i) S/90, (j) SC5/90, (k) SC10/90, and (l) SC15/90.

in a water bath at 37 °C for 20 weeks. The pH value of PBS was measured weekly and then the percentages of weight loss ($\%W_{t\,loss}$) and weight loss rate ($\%W_{t\,loss}$ rate) of the samples were calculated by Eqs. (3) and (4):

$$\%W_{t\,loss} = \frac{W_0 - W_t}{W_0} \tag{3}$$

$$\%W_{t\,loss} = \frac{(\%W^i_{t\,loss} - \%W^{i+1}_{t\,loss})/\%W^i_{t\,loss}}{14} \tag{4}$$

where $\%W^i_{t\,loss}$ is the percentage of weight loss after any given two weeks, i, W_0 is original dry weight, and W_t is dry weight at t (Imani, Rafienia, & Sh, 2013; Weir, Buchanan, Orr, Farrar, & Dickson, 2013; Zuh, Cooper, Chen, & Niu, 2013).

2.9. Cell proliferation assay

According to the previously published report (Bonakdar et al., 2010), chondrocytes were isolated from articular cartilage of white New Zealand rabbits, and maintained in Dulbecco's Modified Eagles Medium (DMEM)/Ham's F12 growth medium, and supplemented with 100 U/ml penicillin, 100 μg/ml streptomycin (Sigma, USA), and 10% fetal bovine serum (Seromed, Germany).

Cell proliferation rate was evaluated directly on each sample (1.8 cm^2) in 1, 4, and 7 days using 3-(4, 5-dimethylthiazol-2-yl)-2, 5-diphenyltetrazolium-bromide (MTT, Sigma, USA) assay. All the experiments were performed three times and 24 well tissue culture plates (Orange Scientific, Belgium) were considered as controls. Ten thousand cells in a 50 μl drop of medium were cultured on each sample and incubated at 37 °C. After 3 h, 1 ml medium was added to each sample and then incubation was continued. At each specific time, the medium was removed and replaced by 100 μl of MTT solution (0.5 mg/ml) in PBS. After 4 h, purple formazan crystals were dissolved in 100 mL isopropanol (Merck, Germany) and transferred to an empty tissue culture plate. The absorbance of each well was measured by a multi well microplate reader (Shimadzu, 1601) at 545 nm, and normalized to the control measurement.

The morphology of the cultured chondrocytes (3×10^3 cells/cm^2) on each sample was observed by SEM images. After 1, 4 and 7 days of culture, the cells were fixed by glutaraldehyde solution (4%, Merck, Germany) in PBS for 24 hours at 4 °C. Dehydration process was performed on each specimen in graded alcohols (10%, 30%, 50%, 70%, 80%, 85%, 90%, 95%, and 100%), each for 10 min, then they were sputter-coated with gold, and viewed by SEM.

Table 2
Mechanical properties of composite films.

Sample	Young's modulus (MPa)	Tensile strength (MPa)	Elongation at break (%)	Compression modulus (MPa)	Compression strength at 20% (MPa)
S/70	24 ± 5.5	2.6 ± 0.41	54	10.14 ± 2.3	4.33 ± 0.34
SC5/70	66 ± 3.9	3.61 ± 0.32	51	9.71 ± 2.5	3.18 ± 0.23
SC10/70	82 ± 7.1	3.82 ± 0.55	36	7.76 ± 3.1	2.76 ± 0.41
SC15/70	93 ± 3.6	4.03 ± 0.48	25	6.37 ± 1.4	2.54 ± 0.33
S/90	20 ± 4.2	2.48 ± 0.33	52	7.28 ± 2.8	2.95 ± 0.36
SC5/90	63 ± 2.9	3.58 ± 0.74	50	6.8 ± 3.2	2.82 ± 0.29
SC10/90	81 ± 6.5	3.66 ± 0.42	37	5.75 ± 1.6	2.69 ± 0.31
SC15/90	85 ± 7.5	3.97 ± 0.26	22	5.23 ± 2.2	2.38 ± 0.52

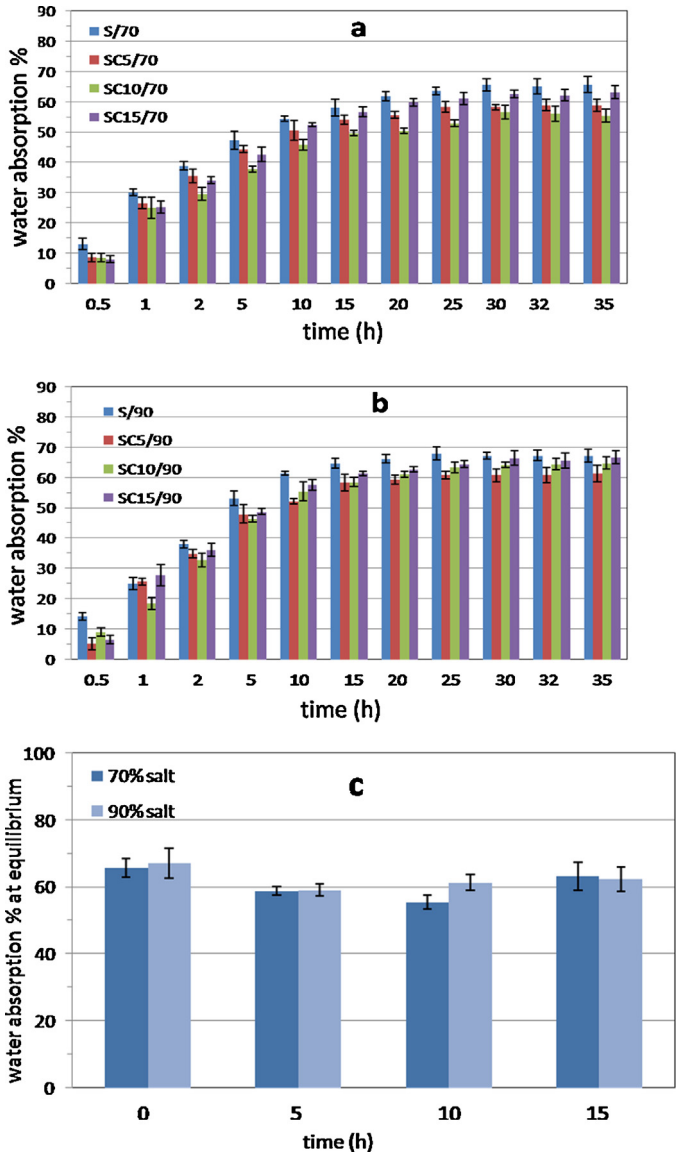

Fig. 2. (a and b) Water uptake profile of the starch based scaffolds obtained by combining the salt leaching and freeze drying methodologies for times of up to 35 h and (c) water absorption percentage at equilibrium of specimens.

2.10. Statistical method

The quantitative data were presented as mean including ±standard errors of the mean ($n = 3$) and analyzed using Student's t-test or one-way ANOVA analysis by SPSS software (version 16.0). The values of $P < 0.05$ were considered statistically significant.

3. Results and discussion

3.1. Morphology study of fibers

Fig. 1a and b shows the SEM pictures of vascular bundles of rice straw cross section and bleached rice straw fibers, respectively. It is clear that chemical purification disintegrates the bundles and decreases the average dimension of fibers to about 5–20 μm and exposes the nano-scale fibers bundles on the surface of microfibers. Fig. 1c shows the FE-SEM image of mechanically treated fibers using sonication. The nanofibers network was defibrillated from micro-sized cellulose fibers after mechanical treatment. The sonication power disintegrates nanofiber bundles by a combination of events, including formation, growth, and collapsing of cavities, called cavitations (Chen, Yu, et al., 2011; Filson & Dawson-Andoh, 2009). The image analysis (UTHSCSA image tool) shows that the nanofibers have suitable diameter dispersion in the range of nanometer. Statistical analysis reveals that 10% of fibers are smaller than 40 nm, 10% are in the range of 40–70 nm, 50% are in the range of 70–90 nm, and 30% of fibers are longer than 90 nm.

3.2. Chemical compositions of fibers

The results of NREL illustrate that untreated fibers have lower cellulose content and higher lignin and hemicelluloses contents compared to alkali treated fibers. The percentage of α-cellulose was increased from 46.5 ± 0.7 to 79.3 ± 0.8, while the fraction of lignin and hemicelluloses was declined from 29.1 ± 0.3 to 15.9 ± 0.2and 22.5 ± 0.6 to 4.8 ± 0.3, respectively, after alkali treatment of rice straw. Due to their amorphous morphology, the chemical penetrates into the structure, causes a breakdown in fiber bundles, hydrolyze hemicelluloses, and depolymerize lignin (Alemdar & Sain, 2008b). In the case of silica content, it was found that the strong alkali treatment with 17.5 wt% NaOH completely removes all the silica content from untreated fibers. It may be attributed to the weak structure and bonding of silica component in the fiber structure (Jahan, Lee, & Jin, 2006).

3.3. Morphology of scaffolds

An ideal scaffold for tissue engineering should have high porous structure and mechanical stability. These two parameters are in conflict with each other. In this study, the effect of nanofibers and salt content on porosity of scaffolds was investigated by porosity test. Fig. 1d shows the porosity percentage for starch based nanocomposite scaffolds at various salt and cellulose nanofibers contents. Porosity is measured by taking the volume of voids over the total volume in a scaffold. Alcohol was used as medium solvent to avoid contraction and collapse of scaffolds caused by air drying. From the results, obviously, porosity would increase with the increase of both salt and cellulose nanofibers content. At the same conditions the porosity increase about 66% for S15/70 compared to S/70, and about 61% for SC15/90 compared to S/90. Also

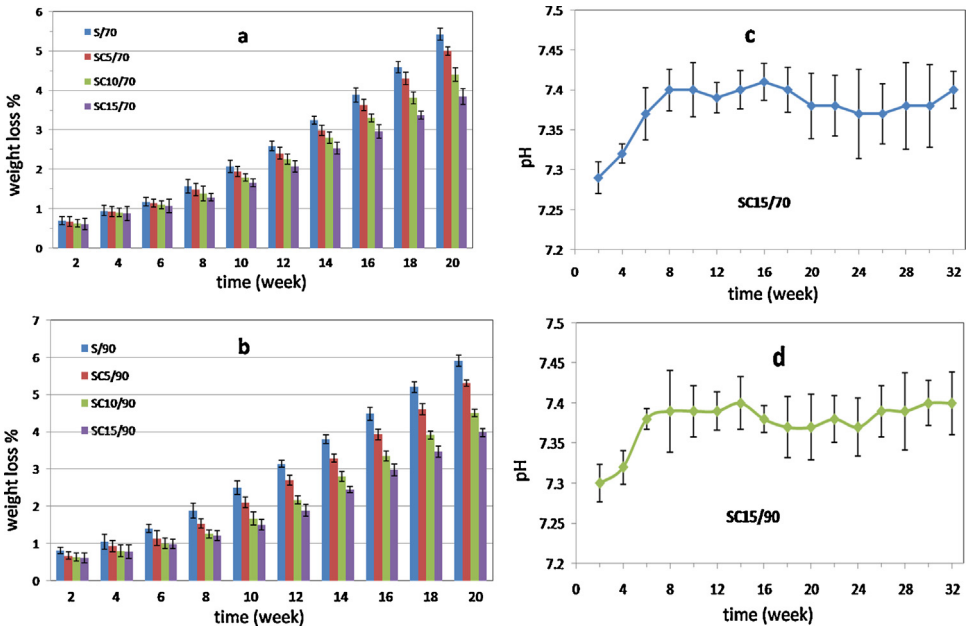

Fig. 3. (a and b) Weight loss percentage profile of the starch based scaffolds in PBS for times of 20 weeks and (c) pH changes trends of SC15/70 and (d) SC15/90 by 32 weeks.

results (Fig. 1d) demonstrate that scaffolds with 90% salt show a noticeable increasing at porosity percent, compared to 70% salt. The cross section SEM images of scaffolds were shown in Fig. 1e-l. The morphology of cross section of scaffolds is varied by increasing the nanofibers content. Clearly, it was seen that S/70 and SC5/70 show smoother surface (Fig. 1e and f), whereas SC10/70 and SC15/70 display a more bumpy structure (Fig. 1g and h). The same observations were obtained in the case of S/90 and SC5/90 compared to SC10/90 and SC15/90 (Fig. 1i-l). The microsized pores in the structure of scaffolds can create a very suitable structure for tissue engineering (Yan et al., 2012). Moreover, increasing the nanofibers content may lead to an improvement in tensile properties of the samples (Alemdar & Sain, 2008a). The salt content is another effective factor in scaffolds morphology. It is indicated by results (Fig. 1d) that the salt leached specimen with 90% salt show a more porous structure than corresponding samples prepared by 70% salt. The pores existence is appropriate for transmission of nutrients and metabolic products for cells during their growth. Also, this structure accelerates the degradation process of scaffold and increases the cell seeding and adhesion (Yan et al., 2012). On the other hand, higher porosity may lead to poor mechanical performance which is not suitable in bone tissue engineering (Chen, Ushida, & Tateishi, 2002; Shokrolahi, Mirzadeh, Yeganeh, & Daliri, 2011).

3.4. Mechanical properties

Table 2 illustrates the mechanical properties of pure starch and nanocomposite scaffolds with 5, 10, and 15 wt% CNF leached by 70% and 90% salt content. Due to its high molecular mobility and weak interaction between chains, starch is a brittle polymer with poor mechanical properties (Fabunmi, Tabil, Panigrahi, & Chang, 2007). Obviously, cellulose nanofibers improved the Young´s modulus and tensile strength of the composite samples. The Young´s modulus of scaffold was enhanced about 287% and 325% for CS15/70 and CS15/90 samples, respectively. Tensile strength was also increased about 55% and 60% for CS15/70 and CS15/90, respectively. However, the elongation at break shows a reasonable decrease (54% and 60%) compared to the pure starch film. The improvement of mechanical properties of starch based nanocomposites may be attributed to very good dispersion of nanofibers and also the formation of rigid hydrogen bonds network between starch and cellulose nanofibers that cause a good stress transfer from matrix to nanofibers (Alemdar & Sain, 2008a,b). Scaffolds for tissue applications are also subjected to compression tensions initially in vivo stages. Porosity and pore structure of scaffold are the most effective factors in compression properties (Hejkants, Van Tienen, & De Groot, 2006). Table 2 shows the behavior of starch based samples at compressive 20%. It is concluded that by increasing porogen (salt) from 70% (w/w) to 90% (w/w), the compressive properties show a noticeable decreasing. As it can be seen, the module was declined about 28% for S/90 and 18% for SC15/90 compare to S/70 and SC15/90, respectively. These reductions may be due to density reduction of samples caused by enhancing the porosity (Chen et al., 2002). In addition, by increasing nanofibers from 5 to 15 wt%, a significant decrease in compression properties was observed (Table 2). Although individual nanofibers have high mechanical properties (theoretical Young's modulus 138 MPa and tensile strength 10 GPa) (Nakagaito, Takagi, & Pandey, 2011), agglomeration of cellulose nanofibers at higher contents cause poor performance. At lower nanofibers content, the high modulus and strength of cellulose nanofibers amend the light agglomeration, however, higher nanofibers content might have caused an increase in the heterogeneous porosity of scaffolds and consequently a weak structure (Kaushik, Singh, & Verma, 2010).

3.5. Water absorption behavior of nanocomposites

Water absorption ability can be an important parameter in estimation of fluids uptake from the medium. Therefore, it can be employed as a significant indicator to define the suitability of a biomaterial for tissue engineering. The amount and behavior of water absorption at equilibrium for scaffolds with various nanofiber contents are shown in Fig. 2a–c. For salt leached scaffolds with 70% salt, it was found that by adding CNF up to 10 wt%, the amount of water absorption at equilibrium was reduced about 18.4% compared to the pure starch film. It may be due to the formation of rigid hydrogen bonds network between cellulose and starch (Ghanbarzadeh, Almasi, & Entezami, 2010). However, at higher amounts of cellulose nanofibers (15 wt%), the water absorption of the samples was increased that could enhance the swelling ability of starch-based scaffolds. By increasing the nanofiber contents, the agglomeration of nanofibers leads to enhance the capillary action

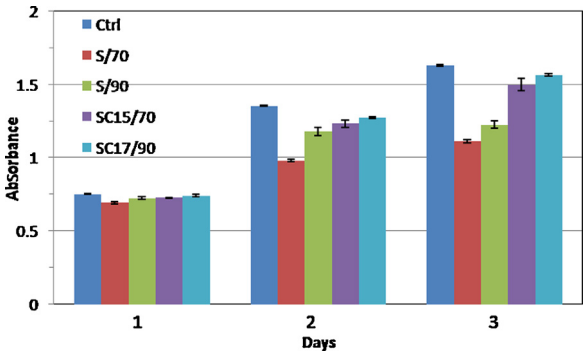

Fig. 4. MTT results of chondrocyte cultured on tissue culture plate (as a control), S/70, S/90, SC15/70, and SC15/90 after 1, 4 and 7 days.

in the composites structure (Phattaraporn, Waranyou, Fazilah, & Thawien, 2010). In the case of 90% salt content, it is observed that by adding 5 wt% nanofibers, water resistance of scaffolds shows a satisfactory enhancing. By further increasing the nanofibers, the water uptake behavior of SC5/90 and SC10/90 was almost the same. The achieved results show the maximum water resistance of samples may be between 5 and 10 wt% nanofibers content. Also, it is observed that the samples with 70% salt have a higher water resistance than the samples with 90% salt which caused by an increase in the water uptake pathway due to the profound salt leaching effect.

3.6. *In vitro degradation*

In vitro degradation of the samples was studied in PBS (pH 7.4) as shown in Fig. 3a and b. All types of scaffolds show a similar weight loss rate after 8 weeks.However, for SC10/70 and SC15/70, slower degradation rate was observed compare to S/70 and SC5/70 scaffolds (Fig. 3a). After 8 weeks, the percentage of $W_{t\ loss}$ rate of S/70, SC5/70, SC10/70, and SC15/70 were obtained to be 0.024, 0.019, 0.018, and 0.01 g/day, respectively. Immersing the composites in PBS led to weak the intermolecular bonding force in starch molecular chains. Therefore, increasing the incubation time causes the fracture of molecular chains. The slower weight loss rate of SC10/70 and SC15/70may be attributed to strong interaction between carbonyl groups of starch and hydroxyl groups of nanofibers and formation of strong hydrogen bonds network which result higher rigidity of composite in comparison to pure starch (Chen, Xi, Zheng, Zhou, & Wan, 2011; Kaushik et al., 2010). A similar result was observed for the samples prepared by 90% salt. It can be seen in Fig. 3b that the percentage of $W_{t\ loss}$ rate of S/90, SC5/90, SC10/90, and SC15/90 are 0.033, 0.028, 0.022, and 0.019 g/day, after 8 weeks. It was demonstrated that the salt leaching by 90% salt did not show a significant effect on degradation rate of starch based scaffolds compared to samples leached by 70% salt. Here, there is a conflict concerning the density of starch cell walls and the morphology of scaffolds after salt leaching. Clearly, by increasing the salt content, the wall thickness of porosities in matrix decreases, this may be the reason for developing degradation rate in PBS. On the other hand, when salt leaching was carried out on starch-based samples, removing the amorphous regions of starch structure was more probable than crystalline regions. As it is well known, degradation rate of crystalline domain is slower than amorphous regions. Fig. 3c and d shows that the pH value of solution was decreased to around 7.30 after 2 weeks immersing of scaffold. This is due to weak acidity of materials during the scaffold processing. However, by passing 12 weeks this value was increased. Fig. 3c also shows the variation of pH value of scaffolds (SC15/70 and SC15/90) after 12 weeks. It is due to reduction of weight loss rate and naturalization of little degraded products in PBS (Chen, Yu, et al., 2011). During 8–32weeks, the pH value was fluctuated in a narrow range from 7.37 and 7.41. There is no significant variation ($P > 0.05$) during this time due to a decline in degradable products in the solution.

3.7. *Cytocompatibility*

In order to evaluate the toxicity of the samples, MTT assay was performed three times on each sample according to the previously published report (Bonakdar et al., 2010). The extraction procedure was carried out based on ISO 10993-12 instruction in which each sample with 1.8 $cm^2$was exposed to 50 μl culture medium. The same medium was considered as control. Fig. 4 shows the results of cell proliferation assay which indicates no more than 90% viability

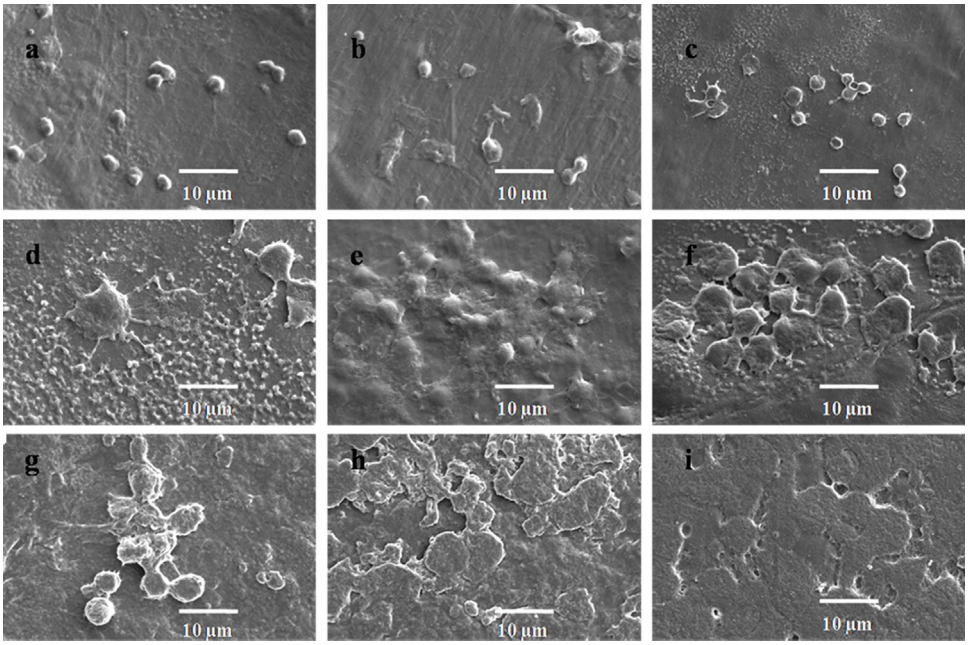

Fig. 5. The morphology of chondrocyte cells cultured on the samples (a) S/90, (b) SC15/70 and (c) SC15/90 after 1 day, (d) S/90, (e) SC15/70 and (f) SC15/90 after 4 days, and (g) S/90, (h) SC15/70 and (i) SC15/90 after 7 days of cell seeding.

for all the samples in comparison to control. It can be observed that SC15/70 and SC15/90 stimulate the proliferation rate of the cells after 4 days. This can prove the inductive role of cellulose nanofibers for cell attachment and proliferation.

3.8. Cell–scaffolds interaction

The interaction of chondrocytes with the prepared scaffolds was studied after 1, 4 and 7 days following cell seeding. The SEM micrographs of the cells were recorded to study the cells spreading and attachment on the samples (Fig. 5). Typically, the scaffold surface was covered with cells. Higher cell attachment at day 1st, well spreading at day 4th, and full coverage at day 7th were achieved by incorporation of nanocellulose into starch matrix. SEM images also confirmed the results of MTT assay. Chondrocytes showed a rounded morphology on SC15/70 and SC15/90 scaffolds after 4 days of culture. The cells were well attached to the substrate with the formation of filopodia which demonstrated the appropriate interaction and adequate connection with scaffolds. The compressive elastic modulus of the SC15/70 and SC15/90 samples were in the range of compressive modulus of human articulate cartilage (1.9–14.4 MPa) (Stammen, Williams, Ku, & Guldberg, 2001) which makes them suitable for chondrocyte cell seeding. In addition, MTT analysis revealed that the samples did not have any toxicity. Considering these optimistic points, these two kinds of scaffolds show appropriate properties for attachment, proliferation, and tendency to form colony from chondrocyte cells (Fig. 5h and i).

4. Conclusion

In this work, three-dimensional starch/cellulose nanofibers scaffolds with interconnected pores were fabricated using film casting, salt leaching, and freeze drying methods. The chemo-mechanical method was employed to extract cellulose nanofibers from the rice straw with the diameter in the range of 40–90 nm. Clearly, addition of 15% cellulose nanofibers improved the Young's modulus about 287% and 325%, and tensile strength about 55% and 60% at 70% and 90% salt, respectively. Also addition of 15% cellulose nanofibers declined the compression modulus about 59% and 39%, and compression strength about 70% and 24% at 70% and 90% salt, respectively. Agglomeration of nanofibers plays an important role in enhancing the hydrophilicity of the scaffolds. All types of scaffolds showed a similar rate of weight loss after 8 weeks of degradation, however, degradation rate of the samples prepared by 90% salt was more than the samples prepared by 70% salt due to its morphology change of the samples. Also, the morphology of the nanocomposites varied depending on the initial content of nanofibers and salt. The MTT assay tests and SEM images confirmed the ability of the scaffolds, with interconnected pores, to support and grow fibroblast cells. These starch/cellulose scaffolds offer anew potential for tissue engineering matrix with uniform porous structure, suitable pore size, mechanical properties, and good biodegradability.

References

Ahearne, M., Yang, Y., & Liu, K. K. (2008). In N. Ashammakhi, R. Reis, & F. Chiellini (Eds.), *Mechanical Characterization of Hydrogels for Tissue Engineering Applications*.

Alemdar, A., & Sain, M. (2008a). Biocomposites from wheat straw nanofibers: Morphology, thermal and mechanical properties. *Composite Science and Technology*, *68*(2), 557–565.

Alemdar, A., & Sain, M. (2008b). Isolation and characterization of nanofibers from agricultural residues–Wheat straw and soy hulls. *Bioresource and Technology*, *99*(6), 1664–1671.

Bhatnagar, A., & Sain, M. (2004). *Isolation of cellulose nanofibers from renewable feed stocks and root crops*. University of Toronto.

Bonakdar, S., Hojjati-Emami, S., Shokrgozar, M., Farhadi, A., Hoshiar-Ahmadi, A., & Amanzadeh, A. (2010). Preparation and characterization of polyvinyl alcohol hydrogels crosslinked by biodegradable polyurethane for tissue engineering of cartilage. *Material Science and Engineering*, *30*(4), 636–643.

Chen, C., Ushida, T., & Tateishi, T. (2002). Scaffold design for tissue engineering. *Macromolecule Bioscience*, *2*, 66–77.

Chen, W., Yu, H., Liu, Y., Chen, P., Zhang, M., & Hai, Y. (2011). Individualization of cellulose nanofibers from wood using high-intensity ultrasonication combined with chemical pretreatments. *Carbohydrate Polymers*, *83*(4), 1804–1811.

Chen, Y., Xi, T., Zheng, Y., Zhou, L., & Wan, Y. (2011). In vitro structural changes of nano-bacterial cellulose immersed in phosphate buffer solution. *Journal of Biomimetics, Biomaterials and Tissue Engineering (JBBTE)*, *10*, 55–66.

Elisseeff, J., Puleo, C., Yang, F., & Sharma, B. (2005). Advanced in skeltal tissue engineering with hydrogels. *Orthodontics & Craniofacial Research*, *8*, 150–161.

Elliott, C., & Snyder, G. H. (1991). Autoclave-induced digestion for the colorimetric determination of silicon in rice straw. *Journal of Agriculture and Food Chemistry*, *39*(6), 1118–1119.

Fabunmi, O., Tabil, L., Panigrahi, S., & Chang, P. (2007). *Developing biodegredable plastics from starch*. ASABE, RPV-07130.

Filson, P. B., & Dawson-Andoh, B. E. (2009). Sono-chemical preparation of cellulose nanocrystals from lignocellulose derived materials. *Bioresource Technology*, *100*(7), 2259–2264.

Ghanbarzadeh, B., Almasi, H., & Entezami, A. (2010). Physical properties of edible modified starch/carboxymethyl cellulose films. *Innovative Food Science and Emerging Technologies*, *11*, 697–702.

Hejkants, R. G. J. C., Van Tienen, T. G., & De Groot, J. H. (2006). Preparation of a polyurethane scaffold for tissue engineering made by a combination of salt leaching and freeze-drying of dioxane. *Journal of Materials Science*, *41*, 2423–2428.

Hrabalova, m. (2011). *Viscoelastic and thermal properties of natural fiber-reinforced composites*. Vienna: University of Bodenkultur.

Huang, Y. X., Ren, J., Chen, C., Ren, T. B., & Zhou, X. Y. (2008). Preparation and properties of poly(lactide-co-glycolide) (PLGA)/nano-hydroxyapatite (NHA) scaffolds by thermally induced phase separation and rabbit MSCs culture on scaffolds. *Journal of Biomaterial Applied Science*, *22*, 409–432.

Imani, R., Rafienia, M., & Sh, H.-E. (2013). Synthesis and characterization of glutaraldehyde-basedcrosslinked gelatinas a local hemostat sponge in surgery: An in vitro study. *Bio-Medical and Material Engineering*, *23*, 211–224.

Jahan, M. S., Lee, Z., & Jin, Y. (2006). Organic acid pulping of rice straw. I: Cooking. *Turkish Journal of Agriculture and Forestry*, *30*(3), 1–22.

Kaushik, A., Singh, M., & Verma, G. (2010). Green nanocomposites based on thermoplastic starch and steam exploded cellulose nanofibrils from wheat straw. *Carbohydrate Polymers*, *82*(2), 337–345.

Khademhosseini, A., & Langer, R. (2007). Microengineered hydrogels for tissue engineering. *Biomaterials*, *28*, 5087–5092.

Lu, Y., Weng, L., & Cao, X. (2005). Biocomposites of plastisized starch reinforced with cellulose crystallites from cottonseed linter. *Macromolecul Bioscience*, *5*, 1101–1107.

Nakagaito, A. N., Takagi, H., & Pandey, J. K. (2011). The processing and mechanical performance of cellulose nanofiber-based composites. *International Journal Ocean System Engineering*, *1*(4), 180–184.

Nguyen, K. T., & Jennifer, L. W. (2002). Photopolymerizable hydrogels for tissue engineering applications. *Biomaterials*, *23*, 4307–4314.

NREL. (2008). *Determination of structural carbohydrates and lignin in biomass*. Biomass Program Analysis Technology Team Laboratory Procedure, National Renewable Energy Lab (NREL/TP-510-42618).

Phattaraporn, T., Waranyou, S., Fazilah, A., & Thawien, W. (2010). Characteristic and properties of rice starch films reinforced with palm pressed fibers. *Food Research International*, *17*, 535–547.

Plikk, P., Malberg, S., & Albertsson, A. C. (2009). Design of resorbable porous tubular co-polyester scaffolds for use in nerve regeneration. *Biomacromolecules*, *10*(5), 1259–1264.

Shokrolahi, F., Mirzadeh, H., Yeganeh, H., & Daliri, M. (2011). Fabrication of poly(urethane urea)-based scaffolds for bone tissue engineering by a combined strategy of using compression moulding and particulate leaching methods. *Iranian Polymer Journal-English Edition*, *20*(8), 645–658.

Stammen, J., Williams, S., Ku, D., & Guldberg, R. (2001). Mechanical properties of a novel PVA hydrogel in shear and unconfined compression. *Biomaterials*, *22*(8), 799–806.

Tiexeira, M., Lotti, C., Correa, A. C., Teodoro, B. R., Morcancini, M., & Mattoso, H. C. (2010). Thermoplastic corn starch reinforced with cotton cellulose nanogibers. *Journal of Applied Polymer Science*, *120*, 2428–2433.

Weir, N. A., Buchanan, F. J., Orr, J. F., Farrar, D. F., & Dickson, G. R. (2013). Degradation of poly-L-lactide. Part 2: Increased temperature accelerated degradation. *Journal of Engineering of Medicine*, *218*, 321–330.

Wool, R. P., & Sun, X. S. (2005). *Bio-based polymers and composites*. London: Elsevier Science & Technology Books.

Yan, L. P., Oliveira, J. M., Oliveira, A. L., Caridade, S. G., Mano, J. F., & Reis, R. L. (2012). Macro/microporous silk fibroin scaffolds with potential for articular cartilage and meniscus tissue engineering applications. *Acta Biomaterialia*, *8*(1), 289–301.

Zhang, Y., Fan, W., Ma, Z., Wu, C., Fang, W., & Xiao, Y. (2010). The effects of pore architecture in silk fibroin scaffolds on the growth and differentiation of BMP7-expressing mesenchymal stem cells. *Acta Biomaterialia*, *6*(8), 3021–3028.

Zuh, N., Cooper, D., Chen, X. B., & Niu, C. H. (2013). A study on thein vitro degradation of poly(L-lactide)/chitosan microspheres scaf folds. *Frontiers of Materials Science*, *7*, 76–82.